

Are your **MRI contrast agents** cost-effective?

Learn more about generic **Gadolinium-Based Contrast Agents**.



FRESENIUS
KABI

caring for life

AJNR

Intracranial hemorrhage in premature infants: sonographic-pathologic correlation.

D S Babcock, K E Bove and B K Han

AJNR Am J Neuroradiol 1982, 3 (3) 309-317

<http://www.ajnr.org/content/3/3/309>

This information is current as
of April 17, 2024.

Intracranial Hemorrhage in Premature Infants: Sonographic-Pathologic Correlation

D. S. Babcock¹
K. E. Bove²
B. K. Han¹

Spontaneous intracranial hemorrhage is the most common central nervous system abnormality in premature infants. In this report the cranial sonographic and pathologic findings of 25 autopsied premature infants are correlated. The presence and size of subependymal, intraventricular, and intraparenchymal hemorrhage were well documented by sonography. Cerebellar, choroid plexus, and cortical hemorrhage, though less frequent, were also recognized. There was good correlation as to the presence and degree of hydrocephalus. Prominent subarachnoid spaces on sonography correlated poorly with subarachnoid hemorrhage at autopsy and may be a normal variant in the premature infant. Anoxic brain damage was not diagnosed early by sonography unless associated with hemorrhage, but diffuse brain atrophy with hydrocephalus ex vacuo was detected by sonography.

Spontaneous intracranial hemorrhage is a phenomenon that occurs in premature infants [1-3] and, according to Leech and Kohlen [3], is the most common central nervous system abnormality in neonatal autopsies. The incidence at autopsy in premature infants has been found to be 56%-71%. The hemorrhage usually originates in the subependymal germinal matrix and may extend into the ventricles and the parenchyma.

Until recently, hemorrhage was recognized by clinical methods or cranial computed tomography (CT). In the last several years, B-mode sonography has proven useful and accurate for evaluating hydrocephalus and other abnormalities of the infant brain [4-14]. Recent articles have reported the demonstration of intracranial hemorrhage by sonography and reported good correlation with CT [15-23]. We report the sonographic and pathologic correlation on 25 premature infants examined at our institution during the past 3 years.

Materials and Methods

During the period from April 1978 to December 1980, 28 neonates who underwent cranial sonography subsequently died and were autopsied. The sonograms and autopsy results of these infants were retrospectively reviewed to determine the correlation of the location and size of intracranial hemorrhage and presence and degree of hydrocephalus. Other abnormalities of the brain were also noted. Three patients had either technically inadequate sonographic or pathologic examinations and were excluded, reducing the study group to 25 patients. A sonogram was performed within 24 hr of death in 12 patients, including all of those who died during the first week of life, and 10 of the 13 who died during the first 11 days. Four patients had sonograms within 3 days of death, four within 6 days of death. The remaining five patients died 9 days to 1 month after the last sonogram, but these were infants who died later at 3 weeks to 9 months of age.

Sonography was performed with a mechanical sector real-time scanner (ATL) or a contact scanner (80L Digital, Picker) and a 5.0 or 3.5 MHz transducer. Our sonographic technique for evaluating the infant head has been described in detail elsewhere [11, 24].

Infant brains were removed at autopsy, fixed for several weeks in neutral buffered

Received May 26, 1981; accepted after revision September 16, 1981.

Presented at the annual meeting of the American Roentgen Ray Society, San Francisco, March 1981.

¹Department of Radiology, Children's Hospital Medical Center, Elland & Bethesda Aves., Cincinnati, OH 45229. Address reprint requests to D. S. Babcock.

²Department of Pathology, Children's Hospital Medical Center, Cincinnati, OH 45229.

AJNR 3:309-317, May/June 1982
0195-6108/82/0303-0309 \$00.00
© American Roentgen Ray Society

TABLE 1: Sensitivity, Specificity, and Accuracy of Sonography

Site of Hemorrhage	Accuracy*	Sensitivity†	Specificity‡	False Positive	False Negative
Intracranial	24/25 (96)	20/21 (95)	4/4 (100)	0	1
Subependymal	23/25 (92)	16/18 (89)	7/7 (100)	0	2
Intraparenchymal	24/25 (96)	6/6 (100)	18/19 (94)	1	0
Intraventricular	22/25 (88)	15/18 (83)	7/7 (100)	0	3
Hydrocephalus	22/25 (88)	14/14 (100)	8/11 (73)	3	0
Subarachnoid	15/25 (60)	3/6 (50)	12/19 (63)	7	3

Note.—Numbers in parentheses are percentages.

* Accuracy = (true positives + true negatives)/(true positives + true negatives + false negatives + false positives)

† Sensitivity = true positives/(true positives + false negatives).

‡ Specificity = true negatives/(true negatives + false positives).

formalin, and examined using a conventional coronal sectioning technique. The sections were made at 1 cm intervals.

Results

Sonography demonstrated intracranial hemorrhage at some site in 20 of 21 infants, an accuracy of 96%. The one false-negative patient had blood only in the fourth ventricle, and the site of origin of the hemorrhage was not identified at autopsy. The exact localization of the hemorrhage, however, was not always possible by sonography. In the subependymal hemorrhage group (18 infants), intraventricular hemorrhage was recognized by sonography but the subependymal component was not detected in two cases. Intraventricular hemorrhage (18 cases) was detected when echogenic clot was present in the ventricles and/or when the ventricles were moderately to markedly dilated. In the three false negatives in this group, the ventricles were not dilated and there was minimal blood in the ventricles. Intraparenchymal hemorrhage (six cases) was accurately identified except for one false-positive patient who had periventricular gliosis at autopsy which may have been due to previous hemorrhage but could have been due to other etiologies. There was good correlation as to the presence and degree of hydrocephalus (14 cases). The three false positives had slightly prominent ventricles on sonography and were normal on pathology; we learned that the normal ventricles vary from slits to small fluid-filled structures. Prominent subarachnoid spaces were common on early sonograms, but this finding correlated poorly with the presence of subarachnoid hemorrhage over the cerebrum at autopsy (six cases).

Two patients had cerebellar hemorrhage at autopsy; one with a large cerebellar hemorrhage was diagnosed by sonography. Choroid plexus hemorrhage and cortical hemorrhage were present in one patient each and both were recognized by sonography. Anoxic brain damage with periventricular leukomalacia was not diagnosable early by sonography unless associated with hemorrhage. Diffuse brain atrophy with hydrocephalus ex vacuo, a late manifestation of anoxic brain damage, was detected by sonography. Table 1 summarizes the correlations.

Discussion

Spontaneous intracranial hemorrhage in premature infants usually originates in the subependymal germinal matrix

overlying the head and body of the caudate nucleus lateral to the caudothalamic groove (fig. 1) and sometimes in the choroid plexus (fig. 2). The germinal matrix is a highly vascular tissue and is a source of neuroblasts early in gestation which migrate peripherally during development of the fetal brain to form parts of the cerebral cortex, basal ganglia, and other structures. It is largest at 24–32 weeks of gestation, then diminishes, and is virtually absent in the full-term infant [26]. The vulnerability to subependymal hemorrhage disappears as the spongy matrix tissue involutes.

There are numerous theories of pathogenesis of subependymal hemorrhage, including infarction due to thrombosis of the deep cerebral veins, increased venous pressure, increased arterial pressure, and increased subependymal capillary pressure causing rupture of these fragile vessels [27–29]. Hypoxia, pulmonary disease, acidosis, pneumothorax, administration of excess sodium bicarbonate, and coagulation defects are among the factors that have been associated with subependymal and intraventricular hemorrhage.

The hemorrhage can remain isolated in the subependymal germinal matrix or may rupture through the ependymal lining into the ventricular system. Hydrocephalus may result from obstruction of the cerebrospinal fluid pathway by clot, inflammatory ependymitis, or basilar arachnoiditis.

Although subependymal hemorrhage usually conforms to the distribution of the residual germinal matrix, substantial hemorrhage in the periventricular cerebral white matter often coexists. This devastating lesion may result from direct extension from the germinal matrix, but may also be related to reentry of an intraventricular hemorrhage through damaged ependyma into the white matter or by secondary hemorrhage into foci of ischemic necrosis of white matter. The latter, termed periventricular leukomalacia (fig. 1C), is distinguished pathologically from subependymal hemorrhage on the basis of its bland infarctlike histology, its physical independence of germinal matrix, and its clinical association with shock, sepsis, and congenital heart disease [30, 31]. In fact, periventricular leukomalacia cannot be diagnosed by sonography unless hemorrhage is superimposed or until enough time lapses for cavitation to ensue. The term we have chosen, intraparenchymal hemorrhage, is noncommittal with respect to these issues.

The patients in this study demonstrated a broad spectrum of severity of intracranial hemorrhage and other abnormalities. Subependymal germinal matrix hemorrhage is seen on

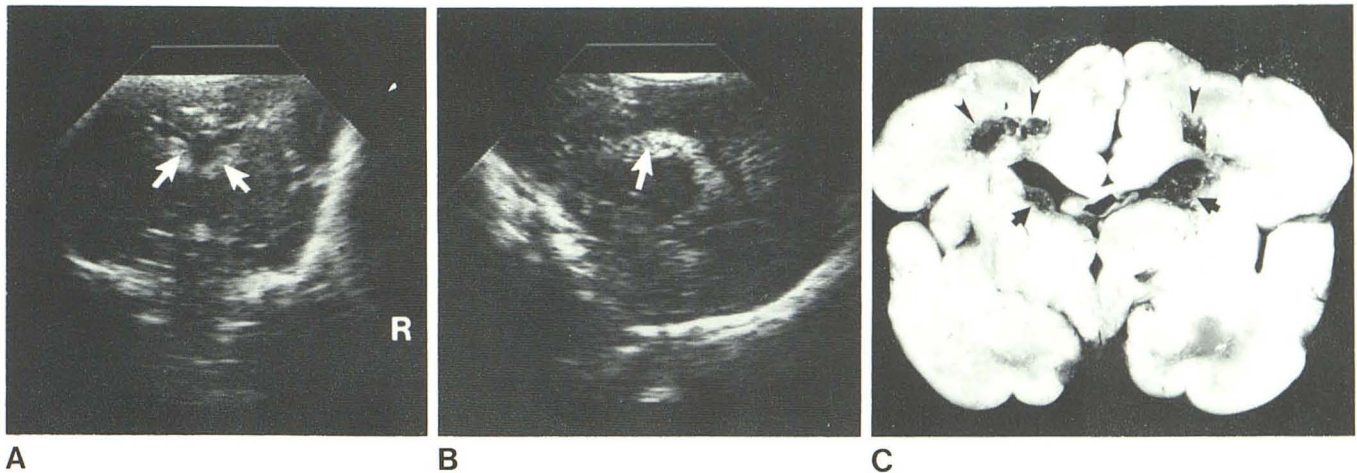
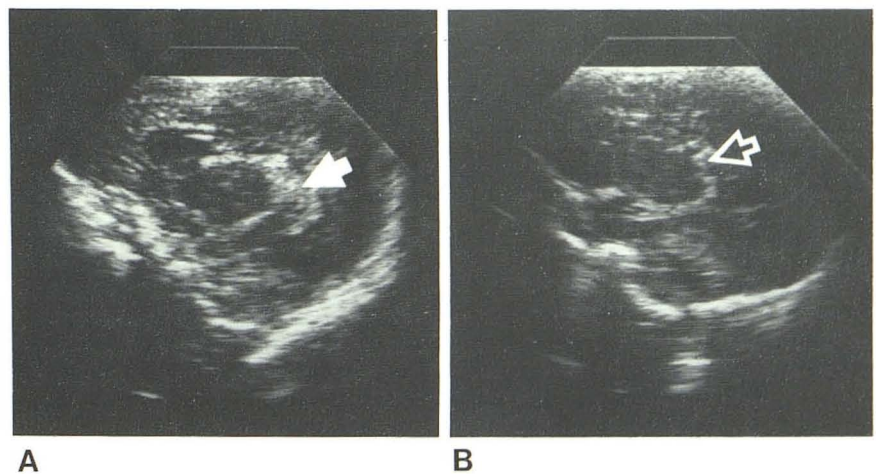


Fig. 1.—Subependymal hemorrhage: 1,320 g, 31-week-gestation infant with respiratory distress syndrome, severe pulmonary interstitial emphysema, and patent ductus arteriosus. Coronal (A) and parasagittal (B) sonograms on day 4 of life. Bilateral small echogenic areas in region of caudate

nucleus representing subependymal hemorrhage (arrows). Ventricles normal size. C. Brain section. Bilateral subependymal hemorrhage (arrows). Periventricular necrosis (arrowheads) not detected by sonography 6 days before death. (Reprinted from [25].)

Fig. 2.—Choroid plexus hemorrhage: 925 g, 32-week-gestation infant with pneumothorax, patent ductus arteriosus, and massive pulmonary hemorrhage. Right (A) and left (B) parasagittal sonograms on day 11 of life. Prominent, more echogenic, right choroid plexus (arrow) compared to left (open arrow) thought to represent choroid plexus hemorrhage. Brain section confirmed.



sonography as increased echogenicity in the wall of the lateral ventricle, usually in the region of the caudate nucleus, which forms the inferolateral wall of the lateral ventricle from the frontal horn to the base of the temporal horn (fig. 1). Normally the caudate nucleus has medium-level echoes similar to those of the surrounding brain parenchyma. A normally highly echogenic structure, the choroid plexus, is also seen in the floor of the lateral ventricle and should not be confused with a subependymal hemorrhage. The choroid plexus is a sharply margined structure and extends posteriorly from the foramen of Monro. The echogenic area in the head of the caudate nucleus anterior to the foramen of Monro that is a frequent site of subependymal hemorrhage should not be mistaken for choroid plexus. Uncommonly, the choroid plexus can also be a source of hemorrhage, and in such cases appears enlarged, irregular in outline, and more echogenic than normal (fig. 2).

The recognition of intraventricular extension of the hem-

orrhage can be made when echogenic clot is seen within the ventricle, forming a clot-fluid level or a cast of the ventricle (figs. 3-7). Since the thin ependymal lining of the ventricle is not identifiable by sonography, it is sometimes impossible to differentiate an intraventricular clot attached to the wall of the ventricle from a large subependymal clot. In our experience, enlargement of the ventricles by anechoic fluid also indicates intraventricular hemorrhage with blood diluted with cerebrospinal fluid.

Extension of the hematoma into the parenchyma is seen as a continuation of this echogenic area into the adjacent cerebral hemisphere, internal capsule, and basal ganglia (figs. 5 and 7). Over a several-week period, the echogenic intraparenchymal hemorrhage becomes partially anechoic with eventual cavitation of that part of the brain (fig. 7).

The ventricles in the normal infant are slitlike or contain a small amount of anechoic fluid, as in our three false positives in the hydrocephalus group. Their angles are sharp and

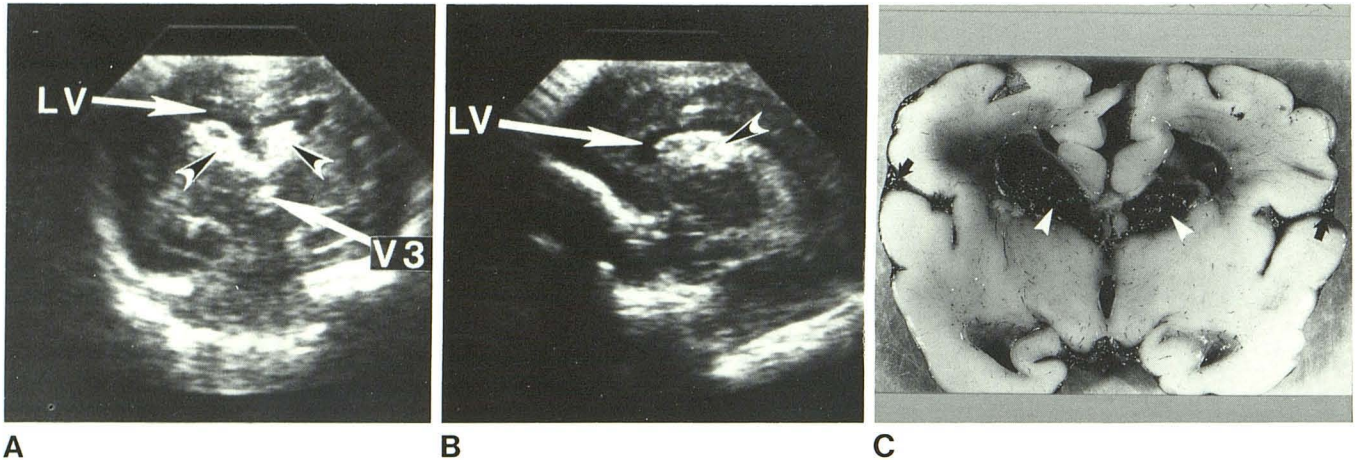


Fig. 3.—Subependymal hemorrhage, intraventricular hemorrhage; mild hydrocephalus, subarachnoid hemorrhage: 1,500 g, 30-week-gestation infant with vertebral, anorectal, tracheoesophageal, and renal anomalies, respiratory distress, and seizures. Coronal (A) and parasagittal (B) sonograms on day 8 of life. Bilateral small subependymal hemorrhages (arrowheads) in region of head of caudate nucleus. Mild ventricular dilatation and echogenic

material within third ventricle (V3) represents intraventricular extension. LV = lateral ventricle. C, Brain section 3 days after last sonographic examination. Intraventricular hemorrhage with bilateral asymmetrical subependymal hemorrhage (arrowheads) and subarachnoid hemorrhage (arrows). (Reprinted from [25].)

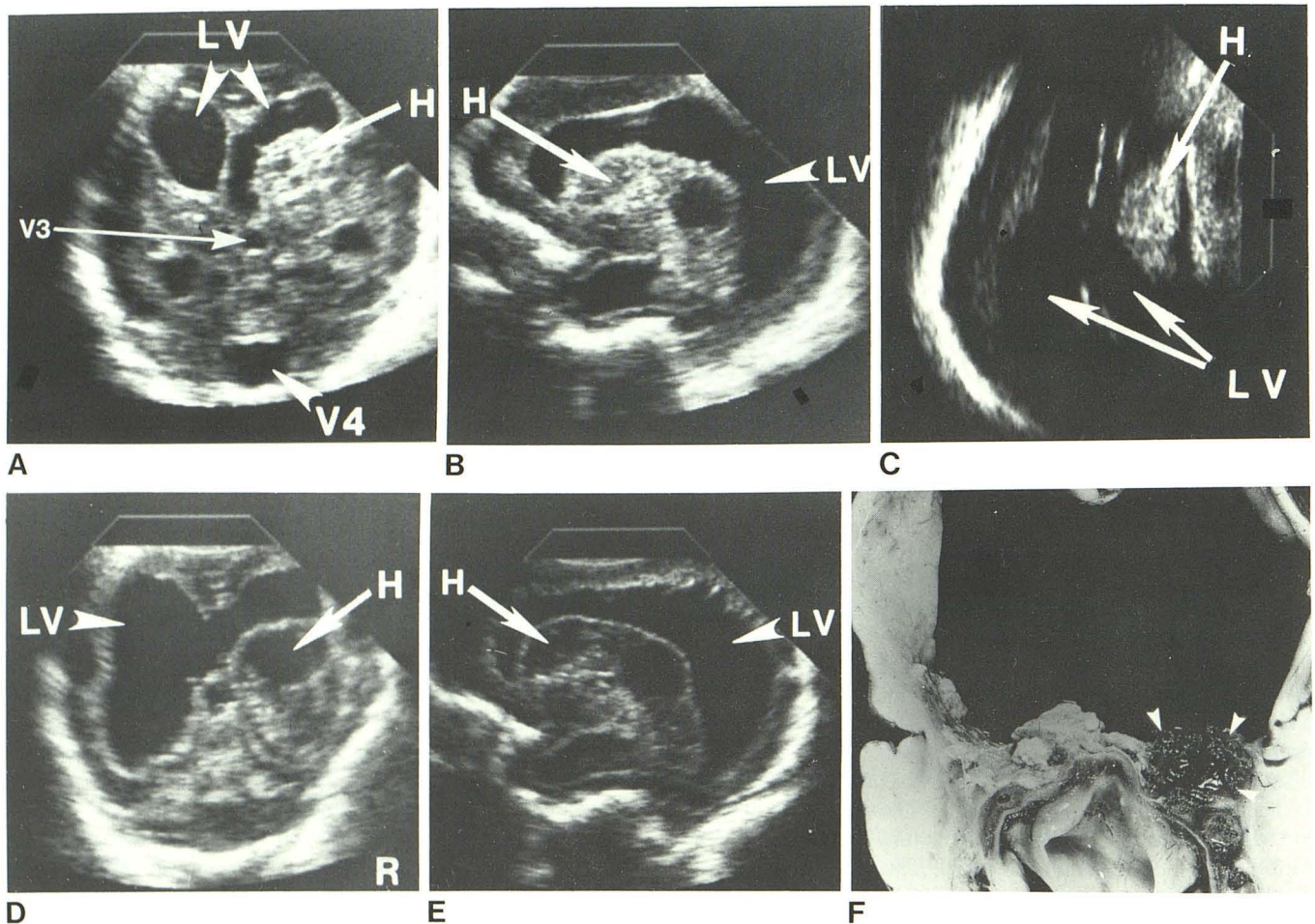
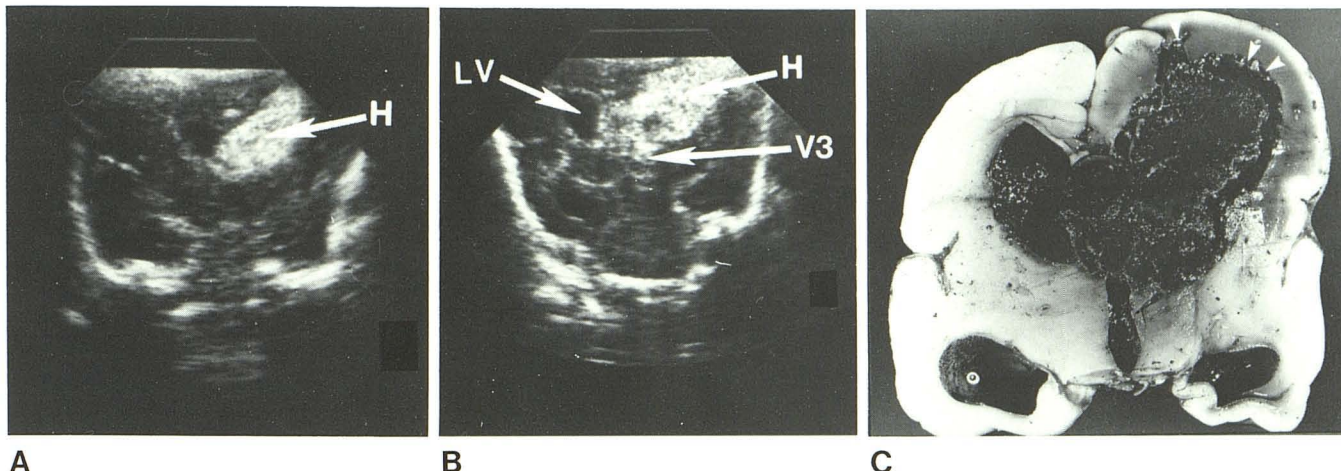


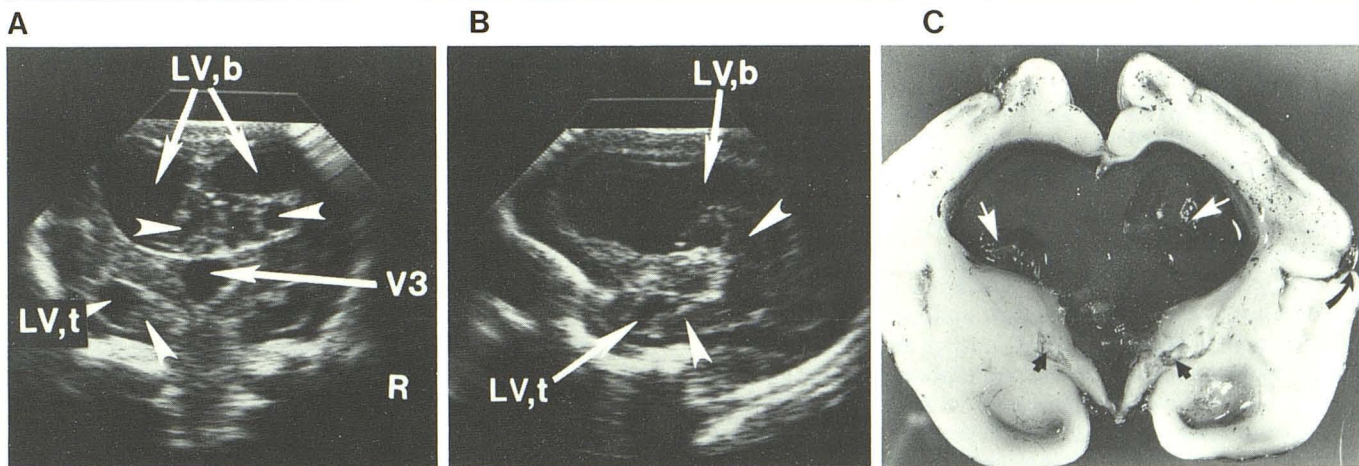
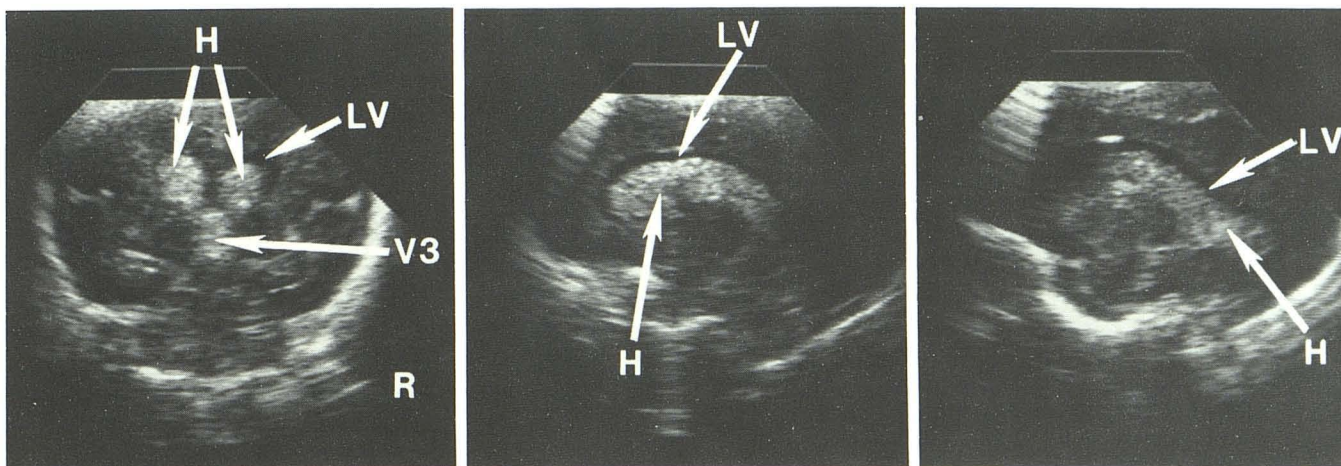
Fig. 4.—Subependymal hemorrhage, intraventricular hemorrhage; massive hydrocephalus: 1,400 g, 32-week-gestation infant with history of birth asphyxia. Increasing head size and drop in hematocrit noted at age 10 days. Coronal (A), right parasagittal (B), and axial (C) sonograms on day 13 of life. Large hematoma (H) on right with marked panhydrocephalus. LV = lateral ventricle; V3 = third ventricle; V4 = fourth ventricle. Coronal (D) and right

parasagittal (E) sonograms 1 week later. Partial liquefaction of hematoma (anechoic areas). Patient died of ventriculitis 2 months later. F, Brain section. Massive panhydrocephalus and residual hematoma (arrowheads) in right caudate nucleus and thalamus. (A, D, and F reprinted from [24]; C, B, and E reprinted from [25].)



A **B** **C**
 Fig. 5.—Subependymal hemorrhage, intraventricular hemorrhage, hydrocephalus, intraparenchymal hemorrhage: 1,110 g, 28-week-gestation infant with severe respiratory distress, pulmonary interstitial emphysema, congestive heart failure, and seizures. **A**, Coronal sonogram on day 3 of life. Right subependymal and intraparenchymal hemorrhage (H). Right lateral ventricle not seen and could be filled by hematoma. **B**, Coronal sonogram 1 week

later. Hematoma on right moderately larger and forms cast of right lateral ventricle. Echogenic material within third ventricle (V3) represents blood. Left lateral ventricle (LV) moderately enlarged. **C**, Brain section 9 days after last sonography. Bilateral subependymal hemorrhage, asymmetrical intraventricular hemorrhage, and multiple foci of intraparenchymal extension (arrowheads).



A **B** **C**
D **E** **F**
 Fig. 6.—Subependymal hemorrhage, intraventricular hemorrhage, hydrocephalus, subarachnoid hemorrhage: 1,440 g, 32-week-gestation infant with respiratory distress, diffuse intravascular coagulopathy, metabolic acidosis, and patent ductus arteriosus. Coronal (**A**) and parasagittal (**B** and **C**) sonograms on day 4 of life. Bilateral hemorrhage (H) in region of caudate nucleus and within dilated lateral (LV) and third ventricles (V3). Coronal (**D**) and

parasagittal (**E**) sonograms 2 weeks later. Ventricles moderately increased with liquifying blood clots (arrowheads). LV,b = body of lateral ventricle; LV,t = temporal horn of lateral ventricle. **F**, Brain section same day as last sonography. Moderate hydrocephalus with blood clots in lateral ventricles (white arrows) and old subarachnoid hemorrhage (curved arrow). Bilateral infarction in globus pallidus (black arrows).

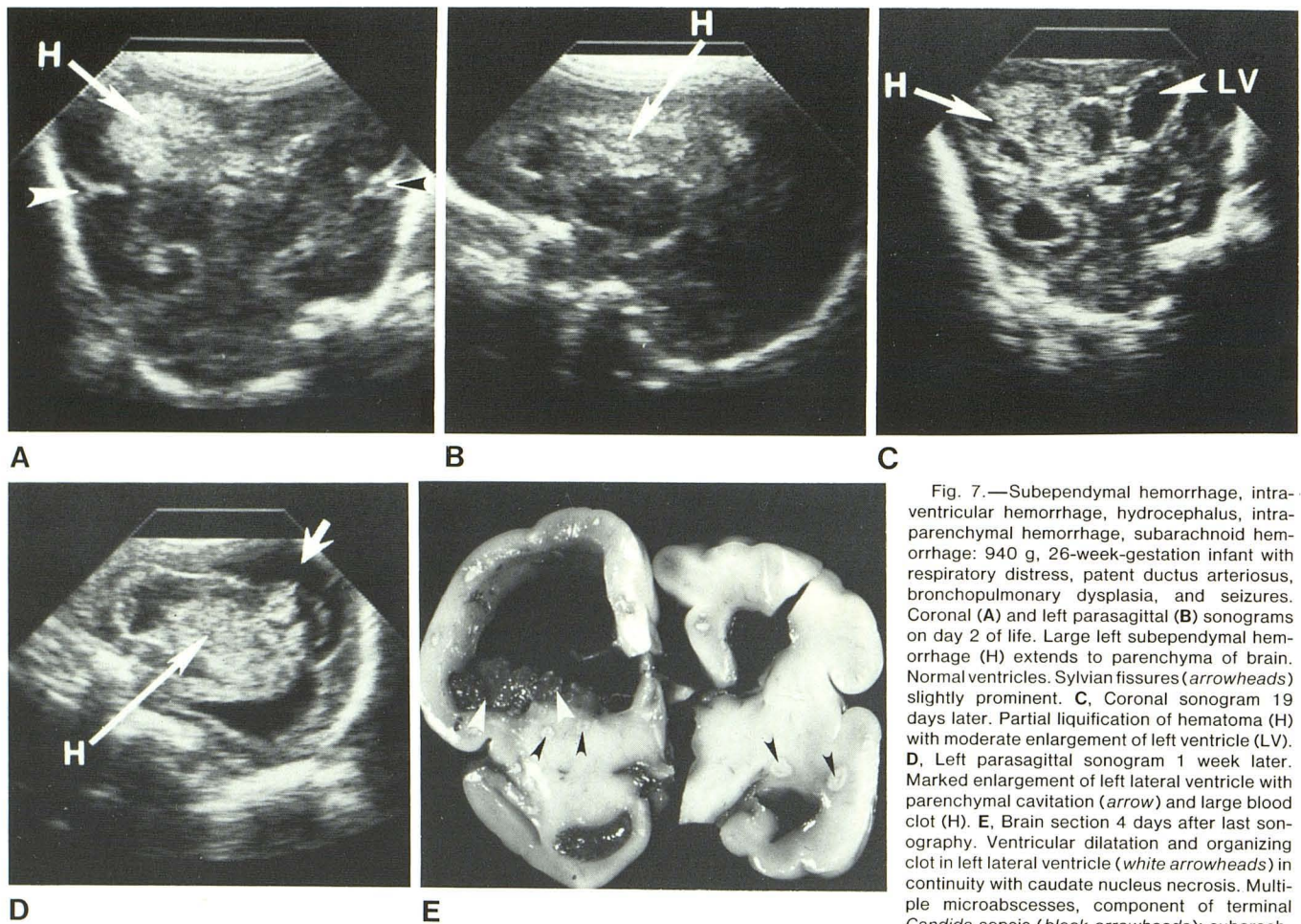


Fig. 7.—Subependymal hemorrhage, intraventricular hemorrhage, hydrocephalus, intraparenchymal hemorrhage, subarachnoid hemorrhage: 940 g, 26-week-gestation infant with respiratory distress, patent ductus arteriosus, bronchopulmonary dysplasia, and seizures. **A**, Coronal and left parasagittal (**B**) sonograms on day 2 of life. Large left subependymal hemorrhage (H) extends to parenchyma of brain. Normal ventricles. Sylvian fissures (arrowheads) slightly prominent. **C**, Coronal sonogram 19 days later. Partial liquefaction of hematoma (H) with moderate enlargement of left ventricle (LV). **D**, Left parasagittal sonogram 1 week later. Marked enlargement of left lateral ventricle with parenchymal cavitation (arrow) and large blood clot (H). **E**, Brain section 4 days after last sonography. Ventricular dilatation and organizing clot in left lateral ventricle (white arrowheads) in continuity with caudate nucleus necrosis. Multiple microabscesses, component of terminal *Candida sepsis* (black arrowheads); subarachnoid hemorrhage.

there is some variation in size, possibly related to the infant's state of hydration. Enlargement of the ventricles beyond the normal was seen and usually correlated with intraventricular hemorrhage in small premature infants. Early dilatation of the ventricles is best seen on coronal and parasagittal views and we found the posterior parts of the lateral ventricles (atria and occipital horns) most sensitive for diagnosing ventricular enlargement.

The sonographic appearance of intracranial hemorrhage varies according to the age of the hemorrhage, much as a hematoma in other locations in the body [32]. Initial examinations demonstrating the hemorrhage showed an area of increased dense echoes. At 2–3 weeks the hematoma became anechoic in its central part indicating liquefaction of the clot which eventually resolved after about 2–3 months. This could be seen with intraventricular clots as well as large subependymal and intraparenchymal hematomas. Cavitation of the brain resulted from large intraparenchymal hematomas (fig. 5). Hemorrhage in other parts of the brain, such as the cerebellum and cortex (fig. 8), were demonstrated.

A prominent extraaxial or subarachnoid space was commonly present on initial sonographic examinations (figs. 7 and 9). This was seen as separation of the brain from the

bony calvarium over the parietal and temporal region and a prominent sylvian fissure. This space disappeared on later examinations and correlated poorly with the presence of subarachnoid hemorrhage over the cerebrum at autopsy. Prominent subarachnoid spaces have been described on CT in premature infants [33] and are thought to be a normal variant in premature infants.

Ischemic brain damage, consisting of periventricular and cortical areas of necrosis or of selective neuronal injury, was seen at autopsy in several of our patients. This was not recognized by sonography, probably because of the small size and nonhemorrhagic character of the lesions resulting in echogenicity similar to that of the adjacent brain. One instance of acute hemorrhagic infarction in the superficial cerebral cortex and one case of late manifestation of ischemic brain damage, diffuse brain atrophy with hydrocephalus ex vacuo, were diagnosed by sonography. In the latter case, the sonographic findings consisted of enlarged ventricles with normal ventricular angles and a prominent interhemispheric fissure and extraaxial spaces. The clinical finding of decreasing or stationary head size confirmed the diagnosis.

The clinical diagnosis of intracranial hemorrhage in premature infants is based on changes in muscular tone and

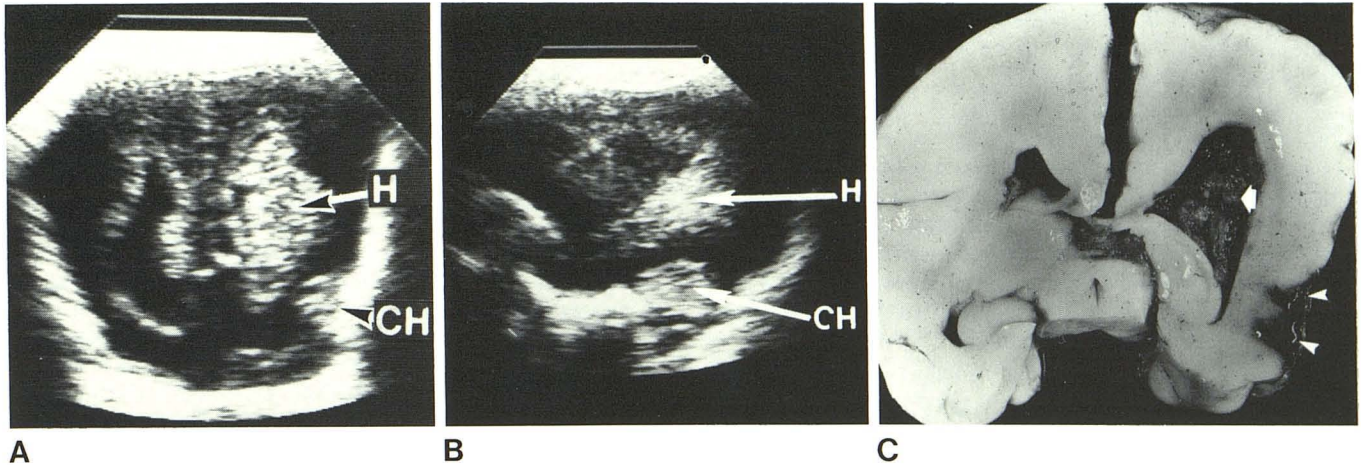


Fig. 8.—Cortical hemorrhage: 700 g, 27-week-gestation infant with respiratory distress, patent ductus arteriosus, episodes of bradycardia, and drop in hematocrit. Coronal (A) and right parasagittal (B) sonograms on day 14 of life. Subependymal hemorrhage (H) extends into brain parenchyma on right.

Lateral ventricles slightly enlarged. Small echogenic area in right temporal lobe represents cortical hemorrhage (CH). C, Brain section 18 days after last sonography. Dilated ventricles. Right lateral ventricle contains clot (arrow). Hemorrhagic infarct in right temporal lobe (arrowheads).

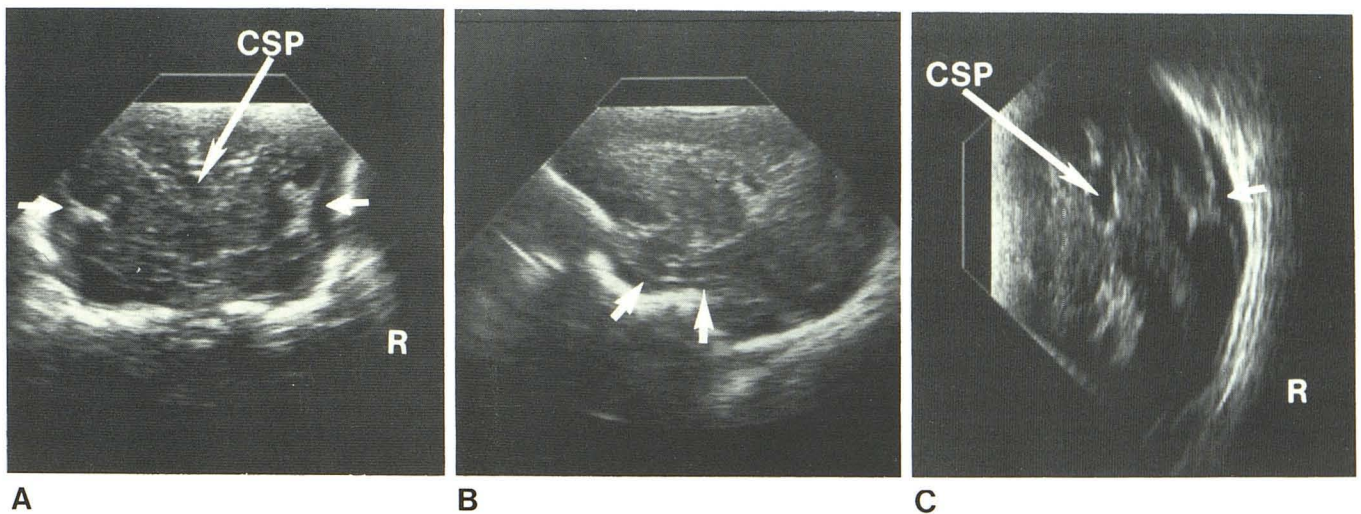


Fig. 9.—Subarachnoid hemorrhage: 1,440 g, 32-week-gestation infant with respiratory distress, diffuse intravascular coagulation, patent ductus arteriosus, and metabolic acidosis. Coronal (A), parasagittal (B), and axial (C) sonograms on day 1 of life. Prominent subarachnoid space (arrows). CSP

= cavum septi pellucidum. Patient subsequently developed subependymal and intraventricular hemorrhage. Brain section showed subependymal hemorrhage, intraventricular hemorrhage, and subarachnoid hemorrhage. (Reprinted from [25].)

activity, seizures, increasing head circumference, bulging anterior fontanelle, hypotension, greater than 10% drop in hematocrit, and blood or elevated protein content in the cerebrospinal fluid. Hydrocephalus is diagnosed by a bulging anterior fontanelle, abnormally increasing head circumference, and transillumination of the head. Prospective studies of intracranial hemorrhage using CT have shown that clinical methods of diagnosis are inaccurate and underestimate its incidence [34–37]. In several studies, cranial computed tomography has been shown to be accurate in diagnosing intracranial hemorrhage in premature infants [35–41].

A recent report has shown transfontanelle real-time son-

ography to be as accurate as CT and more accurate at 7–10 days when hemorrhage may be isodense on CT [19]. The true sensitivity and specificity of an imaging method can be determined by comparing the results of the studies performed shortly before death with the findings at autopsy. Pape et al. [15] reported that the hemorrhage seen on sonography corresponded closely with the degree of intraventricular hemorrhage demonstrated at necropsy in four infants. Mack et al. [42] reported good correlation between sonography and autopsy findings in 12 patients. The evolution of intracerebral hemorrhage in a canine model by sonography, CT, and neuropathology has been described [43]. Our results agree with these studies and support the

conclusion that the diagnosis of intracranial hemorrhage, except for subarachnoid hemorrhage, can be accurately made by sonography.

Sonography has several advantages over CT for diagnosing intracranial hemorrhage. It does not use ionizing radiation and it is noninvasive. The examinations can be performed with portable equipment in the newborn intensive care unit and sedation is not necessary. This is important when dealing with a small, unstable infant when transportation is difficult and dangerous, especially when mechanical ventilation is needed. Also, sonographic equipment and examinations are lower in cost than CT.

Our study shows good sonographic-pathologic correlation on the presence and size of subependymal, intraventricular, and intraparenchymal hemorrhage. There was good correlation as to the presence and degree of hydrocephalus. The normal ventricles were found to vary from slits to small fluid-filled structures. Prominent subarachnoid spaces on sonography correlated poorly with subarachnoid hemorrhage and may be a normal variant in the premature infant. Anoxic brain damage was not diagnosed early by sonography unless associated with hemorrhage. Diffuse brain atrophy with hydrocephalus ex vacuo was detected by sonography.

REFERENCES

- Coen RW, Sutherland JM, Bove K, McAdams AJ. Anatomic and epidemiologic features of the stroke lesion of newborn infants. *Trans Am Neurol Assoc* **1970**;95:36-40
- Tsiantos A, Victorin L, Reiler JP, et al. Intracranial hemorrhage in the prematurely born infant: timing of clots and evaluation of clinical signs and symptoms. *J Pediatr* **1971**;85:854-859
- Leech RW, Kohnen P. Subependymal and intraventricular hemorrhages in the newborn. *Am J Pathol* **1974**;77:465-476
- Garrett WJ, Kossoff G, Jones RFC. Ultrasonic cross-sectional visualization of hydrocephalus in infants. *Neuroradiology* **1975**;8:279-288
- Shkolnik A. B-mode scanning of the infant brain: a new approach. Case report: craniopharyngioma. *JCU* **1975**;3:229-231
- Lees RF, Harrison RB, Sims TL. Gray scale ultrasonography in the evaluation of hydrocephalus and associated abnormalities in infants. *Am J Dis Child* **1978**;132:376-378
- Skolnick ML, Rosenbaum AE, Matzuk T, Guthkelch AN, Heinz ER. Detection of dilated cerebral ventricles in infants. A correlative study between ultrasound and computed tomography. *Radiology* **1979**;131:447-451
- Morgan CL, Trought WS, Rothman SJ, Jimenez JP. Comparison of gray-scale ultrasonography and computed tomography in the evaluation of macrocrania in infants. *Radiology* **1979**;132:119-123
- Johnson ML, Mack LA, Rumack CM, Frost M, Rashbaum C. B-mode echoencephalography in the normal and high risk infant. *AJR* **1979**;133:375-381
- Dewbury KC, Aluwihare APR. The anterior fontanelle as an ultrasound window for study of the brain: a preliminary report. *Br J Radiol* **1980**;53:81-84
- Babcock DS, Han BK, LeQuesne GW. B-mode gray scale ultrasound of the head in the newborn and young infant. *AJR* **1980**;134:457-468
- Johnson ML, Rumack CM. Ultrasonic evaluation of the neonatal brain. *Radiol Clin North Am* **1980**;18:117-131
- Mack LA, Rumack CM, Johnson ML. Ultrasonic evaluation of cystic intracranial lesions in the neonate. *Radiology* **1980**;137:451-455
- Babcock DS, Han BK. Cranial sonographic findings in meningomyelocele. *AJNR* **1980**;1:493-499, *AJR* **1981**;136:563-570
- Pape KE, Cusick G, Houang MTW, et al. Ultrasound detection of brain damage in preterm infants. *Lancet* **1979**;1:1261-1264
- London DA, Carroll BA, Enzmann DR. Sonography of ventricular size and germinal matrix hemorrhage in premature infants. *AJR* **1980**;135:559-564
- Grant EG, Schellinger D, Borts FT, et al. Real-time sonography of the neonatal and infant head. *AJNR* **1980**;1:487-492
- Sauerbrei EE, Harrison PB, Ling E, Cooperberg PL. Neonatal intracranial pathology demonstrated by high-frequency linear array ultrasound. *JCU* **1981**;9:33-36
- Johnson ML, Rumack CM, Mannes EJ, Appareti KE. Detection of neonatal intracranial hemorrhage utilizing real-time and static ultrasound. *JCU* **1981**;9:427-433
- Pape KE, Szymonowicz W, Bennett Britton S, Murphy W, Martin DJ. Ultrasound diagnosis of neonatal intracranial bleeding. In: *Syllabus of the Perinatal Intracranial Hemorrhage Conference, Washington, DC, December 11-13, 1980*. Columbus, OH: Professional Services Department, Ross Labs., **1980**:447-454
- Slovis TL, Shankaran S, Bedard MP, Poland RL. Assessment of intracranial hemorrhage utilizing real time ultrasonic sector scanning as the primary modality: a one-year experience. In: *Syllabus of Perinatal Intracranial Hemorrhage Conference, Washington, DC, December 11-13, 1980*. Columbus, OH: Professional Services Department, Ross Labs., **1980**:536-562
- Bejar R, Curbelo V, Coen RW, Leopold G, James H, Gluck L. Technique for diagnosis and followup of intraventricular and intracerebral hemorrhages by ultrasound studies of the infant's brain through the fontanelles and the sutures. *Pediatrics* **1980**;66:661-673
- Silverboard G, Horder MH, Ahmann PA, Lazzara A, Schwartz JF. Reliability of ultrasound in the diagnosis of intracerebral hemorrhage and posthemorrhagic hydrocephalus: comparison with computed tomographic scan. In: *Syllabus of Perinatal Intracranial Hemorrhage Conference, Washington, DC, December 11-13, 1980*. Columbus, OH: Professional Services Department, Ross Labs., **1980**:501-513
- Babcock DS, Han BK. The accuracy of high resolution real-time ultrasonography of the head in infancy. *Radiology* **1981**;139:665-676
- Babcock DS, Han BK. *Cranial ultrasonography of infants*. Baltimore: Williams & Wilkins, **1981**
- Freide RL. *Developmental neuropathology*. New York: Springer, **1976**:1-37
- Volpe J. Intracranial hemorrhage in the newborn. Current understandings and dilemmas. *Neurology* **1979**;29:632-635
- Hambleton G, Wigglesworth J. Origin of intraventricular hemorrhages in the pre-term infant. *Arch Dis Child* **1976**;51:651-659
- Wigglesworth J, Pape K. An integrated model for haemorrhagic and ischaemic lesion in the newborn brain. *Early Hum Dev* **1978**;2:179-199
- Banker BQ, Larroche JC. Periventricular leukomalacia of infancy: a form of neonatal anoxic encephalopathy. *Arch Neurol* **1962**;7:386-410
- DeReuck J, Chattha AS, Richardson EP. Pathogenesis and evolution of periventricular leukomalacia of infancy. *Arch Neurol* **1972**;27:229-236

32. Wicks JD, Silver TM, Bree RL. Gray scale features of hematomas: an ultrasonic spectrum. *AJR* **1978**;131:977-980
33. Picard L, Claudon M, Roland J, et al. Cerebral computed tomography in premature infants, with an attempt at staging developmental features. *J Comput Assist Tomogr* **1980**;4:435-444
34. Papile LA, Burstein J, Burstein R, Koffler H. Incidence and evolution of subependymal and intraventricular hemorrhage: a study of infants with birth weights less than 1,500 gm. *J Pediatr* **1978**;92:529-534
35. Burstein J, Papile LA, Burstein R. Intraventricular hemorrhage and hydrocephalus in premature newborns: a prospective study with CT. *AJR* **1979**;132:631-635
36. Lee BCP, Grassi AE, Schechner S, Auld PAM. Neonatal intraventricular hemorrhage: a serial computed tomography study. *J Comput Assist Tomogr* **1979**;3:483-490
37. Lazzara A, Ahmann P, Dykes F, Brann AW, Schwartz J. Clinical predictability of intraventricular hemorrhage in preterm infants. *Pediatrics* **1980**;65:30-34
38. Pevsner PH, Garcia-Bunuel R, Leeds N, Finkelstein M. Subependymal and intraventricular hemorrhage in neonates. Early diagnosis by computed tomography. *Radiology* **1976**;119:111-114
39. Krishnamoorthy KS, Fernandez RA, Momose KJ, et al. Evaluation of neonatal intracranial hemorrhage by computerized tomography. *Pediatrics* **1977**;59:165-172
40. Burstein J, Papile L, Burstein R. Subependymal germinal matrix and intraventricular hemorrhage in premature infants: diagnosis by CT. *AJR* **1977**;128:971-976
41. Rumack CM, McDonald MM, O'Meara OW, Sanders BB, Rudikoff JC. CT detection and course of intracranial hemorrhage in premature infants. *AJR* **1978**;131:493-497
42. Mack LA, Wright K, Hirsch JH, et al. Intracranial hemorrhage in premature infants: accuracy of sonographic evaluation. *AJR* **1981**;137:245-250
43. Enzmann DR, Britt RH, Lyons BE, Buxton JL, Wilson DA. Natural history of experimental intracerebral hemorrhage: sonography, computed tomography and neuropathology. *AJNR* **1981**;2:517-526